Shear flow of one-component polarizable fluid in a strong electric field

J. M. Sun* and R. Tao
Department of Physics, Southern Illinois University, Carbondale, Illinois 62901-4401
(Received 28 September 1995)

A shear flow of one-component polarizable fluid in a strong electric field has a structural transition at a critical shear stress. When the shear stress is increased from zero up to the critical shear stress, the flow (in the x direction) has a flowing-chain (FC) structure, consisting of tilted or broken chains along the field (z direction). At the critical shear stress, the FC structure gives way to a flowing-hexagonal-layered (FHL) structure, consisting of several two-dimensional layers which are parallel to the x-z plane. Within one layer, particles form strings in the flow direction. Strings are constantly sliding over particles in strings right beneath. The effective viscosity drops dramatically at the structural change. As the shear stress reduces, the FHL structure persists even under a stress-free state if the thermal fluctuation is very weak. This structure change in the charging and discharging process produces a large hysteresis.

PACS number(s): 82.70.Gg, 61.90.+d, 64.90.+b

I. INTRODUCTION

One-component polarizable fluids are aggregates of particles which can be strongly polarized in an external electric field. The polarization can be either a result of alignment of permanent dipole moments in a field direction, or induced by the electric field as a result of dielectric mismatch between the particles and the medium. The early work in this area could trace back to experiments by Andrade and Dodd [1], who found a significant increase of viscosity for a system of polar molecules in an electric field. Recently, the electrorheological effect exhibited by polymer liquid crystal solutions greatly enhances the interest of research in this area.

A conventional electrorheological (ER) fluid is a two-component fluid consisting of fine dielectric particles in a liquid of low dielectric constant [2]. The large contrast of dielectric constants between the particles and the liquid makes the system easily polarizable in an electric field. The electric-field-induced change of viscosity in ER fluids has provided opportunities for many new technological applications [3–5]. Different from conventional ER fluids, the liquid crystal ER fluid is a one-component polarizable fluid [6–8]. Recent experiments show that liquid crystal ER fluid has significant viscosity enhancement in an electric field and does not sediment. The potential of liquid crystal ER fluids in technological applications is very high. Our present research is to understand the mechanism of this viscosity enhancement and clarify the relationship between viscosity and liquid structure.

In a previous work [9], we examined the viscosity of the one-component polarizable fluids and found three stages in viscosity increase: Newtonian at a weak field, non-Newtonian at an intermediate field, and Bingham plastic with hysteresis at a high field. Our present work is concentrated on the shear flow structure and viscosity in a high field. We will discuss our model and simulation method in Sec. II. In Sec. III, we will report our simulation result. A shear flow of one-component polarizable fluid in a strong electric field has a structural transition at a critical shear stress. When the shear stress is increased from zero up to the critical shear stress, the flow (in the x direction) has a flowing-chain (FC) structure, consisting of tilted or broken chains along the field (z direction). These chains are constantly breaking and rejoining. At the critical shear stress, the FC structure gives way to a flowing-hexagonal-layered (FHL) structure, consisting of several two-dimensional layers which are parallel to the x-y plane. Within one layer, the particles form strings in the flow direction. Strings are constantly sliding over particles in strings right beneath. The effective viscosity drops dramatically at the structural change. During the process to reduce the shear stress, the FHL structure persists even under a stress-free state if the thermal fluctuation is very weak. This structure change in the changing and discharging process produces a large hysteresis.

The layered structure with hexagonal order in ER fluids was also found by Melrose and co-workers [10]. Assuming a uniform shear rate $\dot{\gamma}$ of the base liquid, they concluded that at 10% and 30% volume fraction, the layer hexagonal flow structure was dominant even at a low shear stress, while the aggregate gel structure was at rest. Similar results were also reported by Bonnecaze and Brady [11]. These earlier simulations using constant shear rate boundary conditions cannot simulate the region of gel rupture and by their imposition of constant shear rates always form the FHL structure. They show, however, evidence of the yield stress in that they extrapolate at low shear rates to a dynamic yield stress. In experiments, the ER flow usually does not have a uniform shear rate since the shear flow is induced by a shear force. To avoid such a problem, we do not use this uniform shear rate assumption in our simulation. Instead, we apply a shear force on two particle layers adjacent to the two electrodes that produces a shear flow. From our simulation, we have found that the FC structure at rest is stable up to the critical shear stress.

II. MODEL AND SIMULATIONS

Our three-dimensional system is based on a dipole model [9]. There are N particles placed between two parallel elec-

*Present address: Department of Physics, University of Central Florida, Orlando, FL 32816.

trodes which are planes $z=L/2$ and $z=-L/2$. The motion of each particle is determined by a classical motion equation. The electric force on each particle is the sum of dipolar forces exerted by other particles as well as by images. The flow is moving along the x direction while the applied electric field is along the z direction. In both x and y directions, a periodic boundary condition is imposed.

Based on observations in ER fluid flow experiments that find two layers of dielectric particles cumulated on the two electrodes, we introduce two wall layers adjacent to the electrodes [12]. The particles in the wall layers are distinct from the particles in the flow (bulk particles). While the bulk particles are moving in all directions, the wall layer particles are only moving in the x-y plane and cannot exchange with the bulk particles. Applying a shear force in the x direction to the upper wall layer and a shear force opposite to the x direction to the lower wall layer, we generate a shear flow in Couette geometry.

In our present simulation, we assume that the particles have no permanent dipole moment. In an electric field, each particle obtains an induced dipole moment $\vec{p}=\alpha\epsilon_f(\sigma/2)^3\vec{E}_{\rm loc}$, where $\alpha=(\epsilon_p-\epsilon_f)/(\epsilon_p+2\epsilon_f)$ and $\vec{E}_{\rm loc}$ is the local field. Of course, there is no difficulty to extend our present simulation to particles with permanent dipoles.

The motion of the ith particle is described by a classical motion equation

$$md^2\vec{r}_i/dt^2=\vec{F}_i, \tag{2.1}$$

where $\vec{F}_i$ is the total force acting on it. The dipolar force acting on the particle at $\vec{r}_i$ by a particle at $\vec{r}_j$ is given by

$$\vec{f}_{ij}=\frac{3p^2}{\epsilon_f r_{ij}^4}[\vec{e}_r(1-3\cos^2\theta_{ij})-\vec{e}_\theta\sin(2\theta_{ij})], \tag{2.2}$$

where $\vec{r}_{ij}=\vec{r}_i-\vec{r}_j$ and $0\leq\theta_{ij}\leq\pi/2$ is the angle between z direction and the joint line of the two dipoles. We use $\vec{e}_r$ as a unit vector parallel to $\vec{r}_{ij}$ and $\vec{e}_\theta$ as a unit vector parallel to $\vec{e}_r\times(\vec{e}_r\times\vec{E}_0)$.

A dipole $\vec{p}$ inside the capacitor at $\vec{r}_i=(x_i,y_i,z_i)$ produces an infinite number of images at $(x_i,y_i,-z_i)$ and $(x_i,y_i,2Lk\pm z_i)$ for $k=\pm1,\pm2,\ldots$. The force between a dipole and an image has the same form as Eq. (2.2). The force on the ith particle by the jth particle is given by

$$f_{ij,x}=\frac{p^2}{\epsilon_f L^4}\sum_{s=1}^{\infty}\frac{4s^3\pi^3(x_i-y_j)}{\rho_{ij}}K_1\left(\frac{s\pi\rho_{ij}}{L}\right)\times\cos\left(\frac{s\pi z_i}{L}\right)\cos\left(\frac{s\pi z_j}{L}\right), \tag{2.3}$$

$$f_{ij,y}=\frac{p^2}{\epsilon_f L^4}\sum_{s=1}^{\infty}\frac{4s^3\pi^3(y_i-y_j)}{\rho_{ij}}K_1\left(\frac{s\pi\rho_{ij}}{L}\right)\times\cos\left(\frac{s\pi z_i}{L}\right)\cos\left(\frac{s\pi z_j}{L}\right),$$

$$f_{ij,z}=\frac{p^2}{\epsilon_f L^4}\sum_{s=1}^{\infty}4s^3\pi^3K_0\left(\frac{s\pi\rho_{ij}}{L}\right)\sin\left(\frac{s\pi z_i}{L}\right)\cos\left(\frac{s\pi z_j}{L}\right),$$

where $\rho_{ij}=\sqrt{(x_i-x_j)^2+(y_i-y_j)^2}$ and K_0 and K_1 are the modified Bessel functions. The force on the ith particle by its own images is in the z direction and denoted as $\vec{f}_i^{\rm self}$,

$$f_{i,z}^{\rm self}=\frac{3p^2}{8\epsilon_f}\left[-\frac{1}{z_i^4}+\sum_{s=1}^{\infty}\left(\frac{1}{(z_i-sL)^4}-\frac{1}{(z_i+sL)^4}\right)\right]. \tag{2.4}$$

The short-ranged hard-core repulsive force is approximated by a potential of power law with large n,

$$\vec{f}_{ij}^{\rm rep}\sim\vec{r}_{ij}/r_{ij}^{n+2}. \tag{2.5}$$

It is clear that as n increases, the short-ranged force becomes stronger. The results reported here are related to $n=29$, a value large enough to prevent the particles from collapsing. Now for the bulk particles, $\vec{F}_i$ in Eq. (2.1) is given by

$$\vec{F}_i=\sum_{j\neq i}(\vec{f}_{ij}+\vec{f}_{ij}^{\rm rep})+\vec{f}_i^{\rm self}. \tag{2.6}$$

As mentioned earlier, the wall particles are experiencing additional external force in the x direction which produces the shear flow.

A viscous flow always produces heat which may cause the temperature to rise if the heat is not removed. In our simulations, the temperature in a layer is calculated by the following equation:

$$T=\frac{m}{3k_B(N_l-1)}\sum_{i=1}^{N_l}(\vec{v}_i-\vec{v}_a)^2, \tag{2.7}$$

where N_l is the number of particles in the layer and the average velocity $\vec{v}_a$ is given by

$$\vec{v}_a=\sum_{i=1}^{N_l}\vec{v}_i/N_l. \tag{2.8}$$

To maintain the temperature at a constant T_0, we apply a renormalization procedure to the wall layers and the two layers immediately adjacent to the wall layers,

$$\vec{v}_i^R=\vec{v}_a+(\vec{v}_i-\vec{v}_a)\sqrt{T_0/T}. \tag{2.9}$$

This is equivalent to removing heat in the system from the two electrodes.

In present study, we have $L_x=L_y=28a$ while the distance between the electrodes is $L_z=24a$, where $a=\sigma/2$ is the radius of the particle. Each wall layer contains 50 particles and the bulk has 500 particles. The system has 600 particles in total and a volume fraction 13.4%, which is low enough to make the dipolar model valid. In comparison with our previous study [9], the present system is much larger but the volume fraction remains almost the same. We use a parameter λ to measure the dipolar energy to the thermal energy $\lambda=p^2/(a^3k_BT)$, which also indicates the strength of the electric field [13]. In our simulations, viscosity has a unit of $\sqrt{mk_BT/a^4}$, time has a unit of $\sqrt{ma^2/(k_BT)}$, and shear rate has a unit of $\sqrt{k_BT(ma^2)}$.

We use an algorithm, originally due to Verlet [14], to integrate Eq. (2.1),

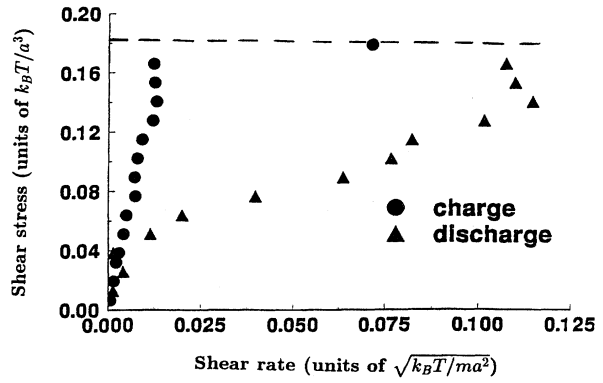

FIG. 1. Shear stress versus shear rate. The dashed line indicates the critical shear stress.

$$\vec{r}_i(t+\Delta t)=-\vec{r}_i(t-\Delta t)+2\vec{r}_i(t)+(\Delta t)^2\vec{F}_i/m+O(\Delta t^4). \tag{2.10}$$

The integration is independent of the velocity. However, the velocity can be determined by

$$\vec{v}_i(t)=\frac{1}{2\Delta t}[\vec{r}_i(t+\Delta t)-\vec{r}_i(t-\Delta t)]+O(\Delta t^2). \tag{2.11}$$

In the layers where heat is removed, the velocity should be renormalized at each step according to Eq. (2.9). Then the positions are given by

$$\vec{r}_i^R(t+\Delta t)=\vec{r}_i(t)+\vec{v}_i^R\Delta t+\frac{1}{2m}\vec{F}_i\Delta t^2. \tag{2.12}$$

The time step in our simulation is $\Delta t=0.01\sqrt{ma^2/(k_BT_0)}$. For a typical liquid crystal ER fluid, $T_0=300$ K, $a=5$ nm, and $m=400\,000$ molecular weight, the time step is about 2×10^{-11} s.

As mentioned earlier, our simulations do not include hydrodynamic interactions and Brownian forces since our model of one-component polarizable does not have a base liquid. The conventional ER fluids are colloid particles in a base liquid which should include all these interactions. However, the full hydrodynamic simulations can only be made on a very small system [11]. The rheology and shear flow behavior derived from our model seem to agree with experimental results of conventional ER fluids [12].

III. RESULTS AND DISCUSSIONS

In our simulations, we take $\lambda=160$. For the above liquid crystal ER fluid, this is equivalent to a dipole moment $p=0.9\times10^{-15}$ cgs unit. To follow an experimental process [15], we first increase the shear stress uniformly in time (charge) and then decrease the shear stress back at the same rate (discharge). By measuring the shear rates, we determine its relationship with shear stress. At one shear stress, we usually run 40 000 time steps, then we increase shear stress by $0.013k_BT/a^3$. Except near the structural transition, 40 000 time steps are long enough for the system to relax. In Fig. 1, we plot the relationship between shear stress and shear rate. In the charge process, the shear rates are generally small, $\dot{\gamma}<0.014\sqrt{k_BT/ma^2}$, when the shear stress is below $0.178k_BT/a^3$. During this charge process, the system has a FC structure.

However, at a critical shear stress $S_c\sim0.178k_BT/a^3$, the shear rate suddenly jumps to a value almost six times the value at the FC structure. At this point, the system undergoes a structure change, from the FC structure to a FHL structure. The dynamics process around the transition point is relatively slow.

The discharge process goes with the same rate to reduce the shear stress. We find the FHL structure persists during the entire discharge process. Since the FHL structure has a much larger shear rate in comparison to the shear rate of the FC structure under the same shear stress, the effective viscosity of the FHL state is much weaker than that of the FC state. Hence we have found a large hysteresis which is associated to the flow structure transition.

A. Flowing-chain structure

The FC structure is characterized by the presence of many chains, tilted in the flow direction. Since the system is in a flow dynamical state, the chains are constantly breaking and rejoining. In Fig. 2, six snapshots are taken of a flow slab. The time interval between two consecutive snapshots is 400 time steps, i.e., $4\sqrt{ma^2/(k_BT)}$. The flow is at a shear stress $0.038k_BT/a^3$ and an average shear rate $0.0027\sqrt{k_BT/ma^2}$. These snapshots clearly show chains are breaking and rejoining in the flow. In the first snapshot, three chains are blackened for identification. In the second snapshot, there is a break at the left chain where three blackened particles have been replaced by the background particles. In the third snapshot, the replaced particles drive three particles out of the center chain. The fourth, fifth, and sixth snapshots show a second break of the left chain, break and rejoin of the center chain, and the right chain. While this flow state has chains breaking, drifting, and rejoining, the basic chain structure always remains.

Figure 3 is a projection of the FC structure on the x-y plane. Each black patch represents a chain along the z direction. Figure 4 shows a projection on the x-y plane of a structure at shear stress close to the critical shear stress S_c. A comparison of these two figures finds that as the shear stress increases, the black patches become prolonged, indicating that the chains are more tilted along the flow direction.

Figure 4 shows that along the x direction the tilted chains begin to form semiconnected strings, which is the precursor of the FHL structure. A further increase of shear stress will force these strings into layers in the x-y direction.

We note that the shear rate $\dot{\gamma}$ fluctuates over time in the FC state because the flow is related to breaking and rejoining of these tightly held chains. A break in one chain generates some increase in $\dot{\gamma}$. When the broken chains rejoin, a relatively stable structure lasts for a while and $\dot{\gamma}$ drops. This is in contrast with the case of a dilute fluid in a weak field where $\dot{\gamma}$ is uniform over time and space [9].

B. Flowing-hexagonal-layer structure

At the critical shear stress S_c, the strings in Fig. 5 aggregate into layers in the x-z plane which have hexagonal lattice structure. Figure 5 is a projection of such a structure in the

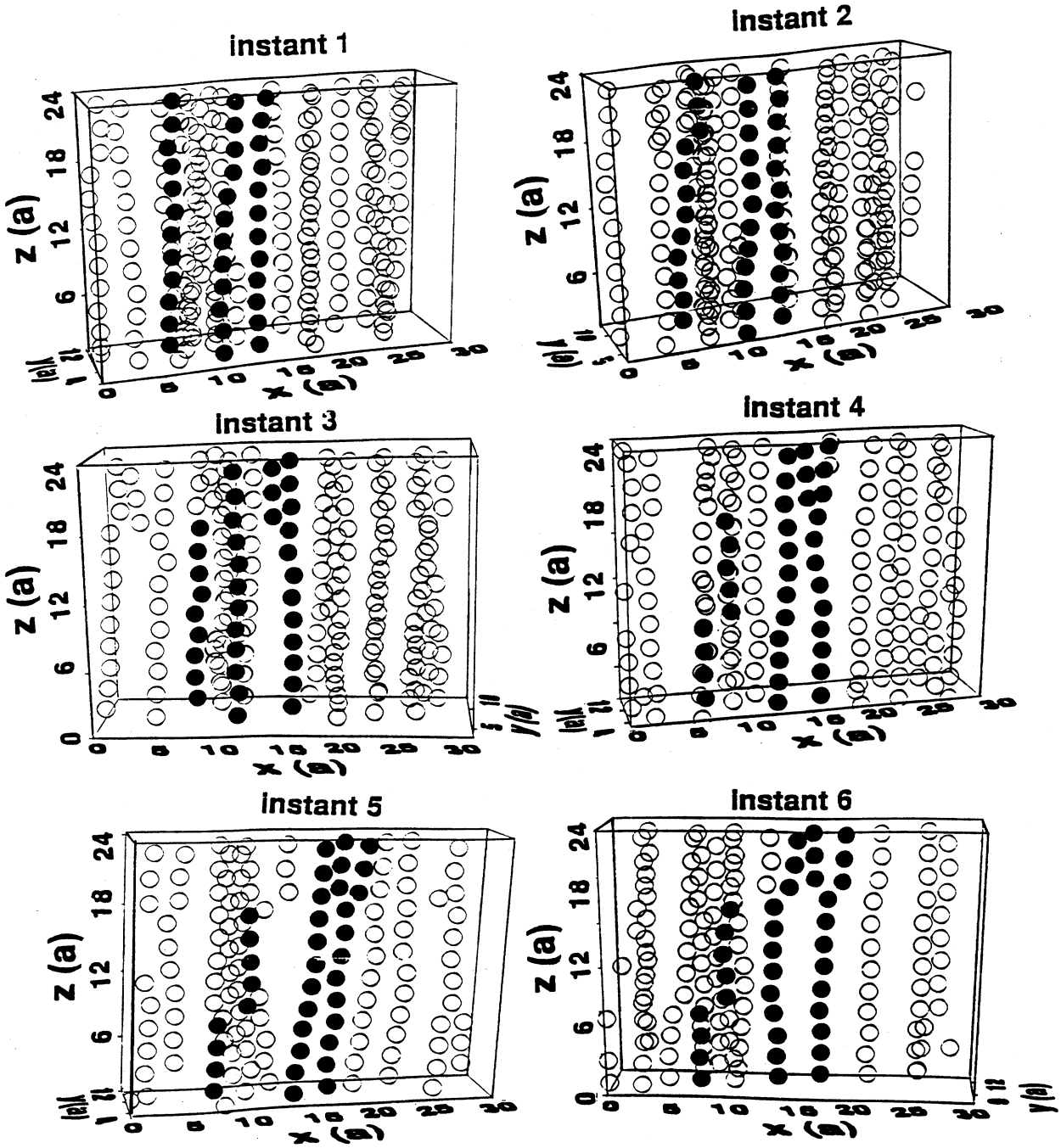

FIG. 2. Six snapshots of a slab of the flow. The time interval between two consecutive snapshots is $4\sqrt{ma^2/k_BT}$. The flow is generated at a shear stress of $0.038k_BT/a^3$ with an average shear rate of $0.0027\sqrt{k_BT/ma^2}$. Under the drive of the shear flow, the chains break into parts, drift, and rejoin while still retaining the basic order of the chain.

x-y plane. The structure is formed at the very onset of structural transition when the shear stress is at S_c. Two layers are seen in Fig. 5 along with several strings which may develop into other layers. As shown in Fig. 6, each layer is a two-dimensional hexagonal lattice in the x-z plane. In this FHL structure the particles form strings in the flow direction, while a string is constantly sliding over particles in a string right beneath. The effective viscosity drops dramatically at the structural change. The FHL flow has a much higher shear rate than the FC flow under the same shear stress. Therefore, the FHL flow is faster than the FC flow under the same shear stress.

In the FHL state, strings slide over each other in the flow direction. Particles are easy to hop from one site to another since the energy barrier between sites is much lower than that in tightly held chains. An examination of Fig. 6 shows

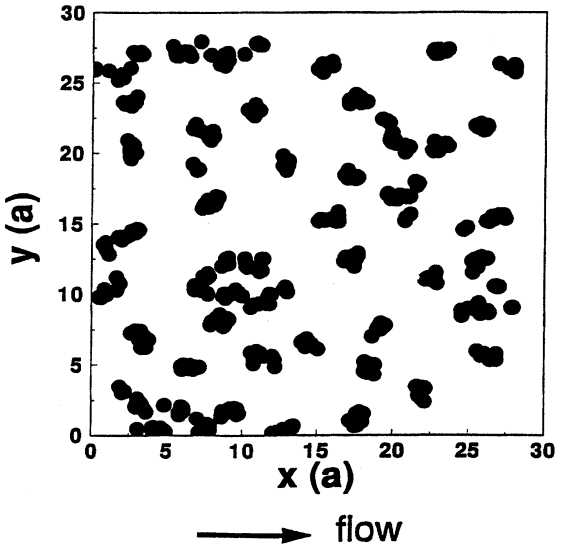

FIG. 3. Projection of the flowing-chain structure on the x-y plane. Each black patch represents a chain in the z direction. The shear stress is $0.038k_BT/a^3$ and the shear rate is $0.0027\sqrt{k_BT/ma^2}$.

that a number of particles are just in a position shifting from site to site. In the FHL flow, the shear rate $\dot{\gamma}$ does not fluctuate as in the FC flow.

Formation of the FHL structure is a slower process than formation of the FC structure. In our simulation, the change process from chains to layers takes a long period after the initial transition. Figure 7 is a projection of a fully developed FHL structure on the x-y plane at a shear stress $0.102k_BT/a^3$ and shear rate $0.077\sqrt{k_BT/ma^2}$.

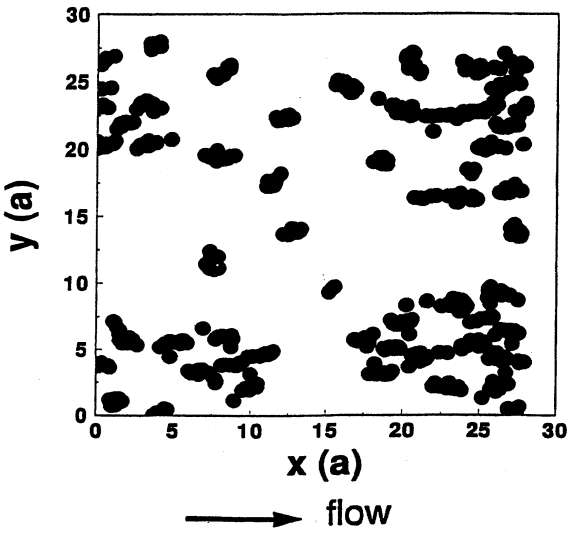

FIG. 4. Projection of the flowing-chain structure on the x-y plane. The shear stress is $0.140k_BT/a^3$ and the shear rate is $0.0130\sqrt{k_BT/ma^2}$. In comparison with Fig. 3, the black patches are prolonged, indicating the chains are more slanted.

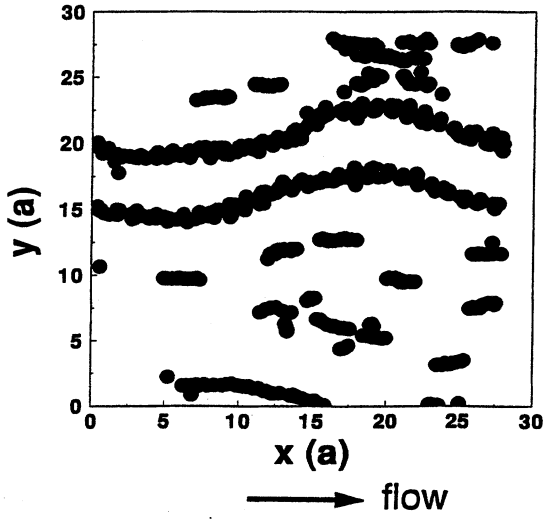

FIG. 5. Projection of the initial formation of the FHL structure at critical shear stress $S_c \sim 0.178k_BT/a^3$ on the x-y plane. The shear rate is $0.0716\sqrt{k_BT/ma^2}$. Two layers are formed.

The FHL flow has been found to persist during the entire discharge process, even when the shear stress goes to zero. Under the stress-free condition, the hexagonal layer structure stays as long as 80 000 time steps, i.e., 1.6 μs. If there is no strong thermal fluctuation, the hexagonal layer structure may stay longer, indicating that the hexagonal layer structure is a metastable state.

To clarify the issue, we consider a class of two-dimensional symmetric structures in Fig. 8(a). These structures have an isosceles triangle ABC as a half primitive cell. If $AB=AC=2a$, that is, particle A and particle B are in contact, the angle θ is restricted to $30°\leq\theta\leq 60°$ because of the hard-core interaction between particles. The hexagonal lattice in Fig. 6 has $\theta=58.6°$ and average $AB=AC=2.15a$, which is very close to a hexagonal lattice with $AB=AC=BC=2a$. The small deviation is due to the fact that the FHL flow has strings of particles constantly sliding over par-

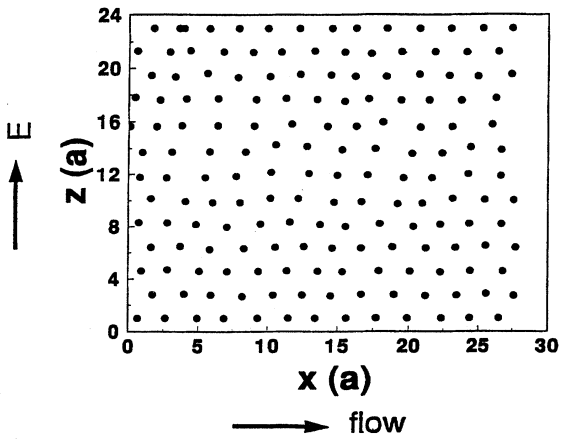

FIG. 6. One x-z layer of the FHL structure, showing the hexagonal ordering.

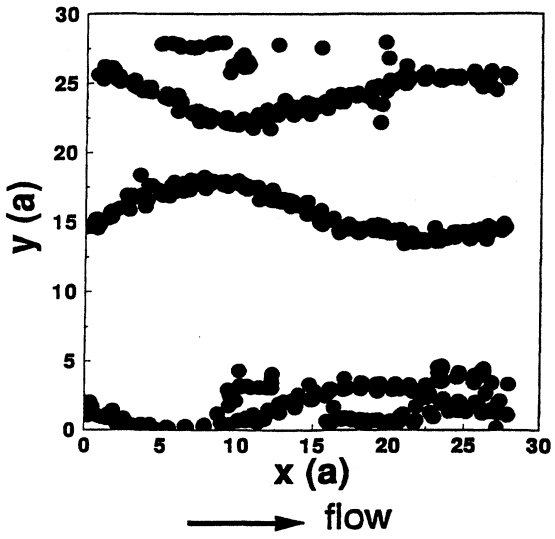

FIG. 7. Projection of a fully developed FHL structure of the x-y plane. The shear stress and shear rate are $0.102k_BT/a^3$ and $0.077\sqrt{k_BT/ma^2}$, respectively. Three layers are formed.

ticles beneath. The structure of $\theta=30°$ is a two-dimensional close-packed chain structure which has chains in the field direction and bears similarity to the three-dimensional body-centered tetragonal (bct) lattice. Though the three-dimensional bct lattice has been proved to be the ground state [16], the dipolar energy per particle of the two-dimensional lattice as a function of θ has two local minima as shown in Fig. 8(b). In fact, because of the symmetry, the dipolar energy per particle in any two-dimensional close-packed hexagonal lattice in the x-z plane is equal. Therefore, we have $u_{\theta=30°}=u_{\theta=60°}=-0.3448(p^2/a^3)$. Although this energy is higher than the dipolar energy per particle in the bct lattice, $-0.381\,268(p^2/a^3)$, it requires a sufficient strong thermal fluctuation to destroy the two-dimensional structure in order to develop the three-dimensional bct lattice once the system is already in the hexagonal lattice of $\theta=60°$.

In conclusion, we note that the FHL structure is obtained under a strong shear stress and the FHL flow has a shear rate nearly uniform over time. For the typical liquid crystal ER fluid mentioned above, this critical shear stress is about 5895

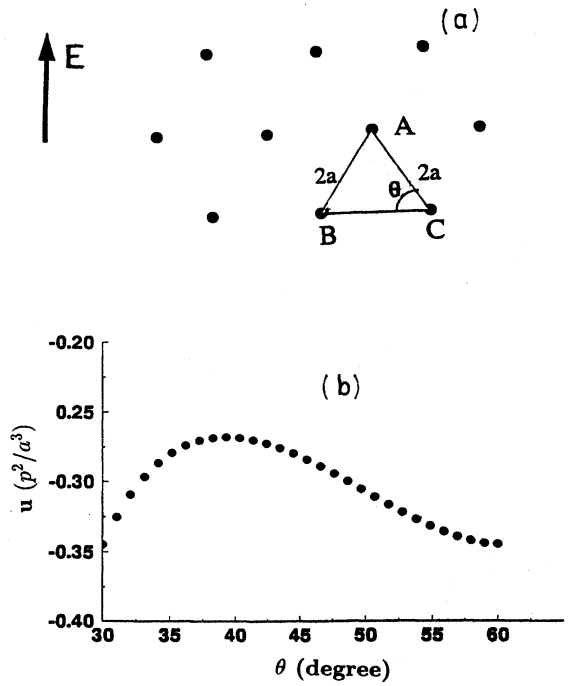

FIG. 8. (a) Two-dimensional structure with an isosceles triangle ABC. $AB=AC=2a$ and $30°\leq\theta\leq60°$. The structure of $\theta=30°$ is a two-dimensional close-packed chains in the field direction. The structure of $\theta=60°$ is the flowing-hexagonal layer. (b) The dipolar energy per particle of the two-dimensional lattice as a function of θ shows a minimum at both $\theta=30°$ and $\theta=60°$.

Pa, which is right in the range of experimental test. If the particle volume fraction is higher, we expect the critical shear stress gets higher, too. We also note that the FC structure is a continuation from the equilibrium structure. The shear rate $\dot{\gamma}$ in the FC flow is not uniform and fluctuates quite a lot over time.

ACKNOWLEDGMENTS

This research is supported by a grant from Naval Surface Warfare Center and a grant from Illinois Consortium for Advanced Radiation Sources.

[1] E. N. Andrade and C. Dodd, Proc. R. Soc. London Ser. A **187**, 296 (1946); **204**, 449 (1951).
[2] For example, see *Electrorheological Fluids*, edited by R. Tao and G. D. Roy (World Scientific, Singapore, 1994).
[3] H. Block and J. P. Kelly, US Patent No. 4 687 589 (1987).
[4] F. E. Filisko and W. E. Armstrong, US Patent No. 4 744 914 (1988).
[5] R. Tao, J. T. Woestman, and N. K. Jaggi, Appl. Phys. Lett. **55**, 1844 (1989).
[6] I. K. Yang and A. D. Shine, J. Rheol. **36**, 1079 (1992).
[7] A. Inoue and S. Maniwa, J. Appl. Polymer Sci. **55**, 113 (1995).
[8] I. K. Yang and A. D. Shine, Macromolecules **26**, 1529 (1993).
[9] J. M. Sun and R. Tao, Phys. Rev. E **52**, 813 (1995).
[10] J. R. Melrose, Phys. Rev. A **44**, R4789 (1991); Mol. Phys. **76**, 635 (1992); J. R. Melrose and D. M. Heyes, J. Chem. Phys. **98**, 5873 (1993).
[11] T. Bonnecaze and J. F. Brady, J. Chem. Phys. **96**, 2183 (1992).
[12] W. T. Ashurst and W. G. Hoover, Phys. Rev. A **11**, 658 (1975).
[13] R. Tao and Q. Jiang, Phys. Rev. Lett. **73**, 205 (1994).
[14] L. Verlet, Phys. Rev. **159**, 98 (1967).
[15] E. Lamaire, G. Bossis, and Y. Grasselli, Langmuir **8**, 2957 (1992).
[16] R. Tao and J. M. Sun, Phys. Rev. Lett. **67**, 398 (1991).